correlation effects will be to uniformly stabilize the twisting potential of the triplet state relative to that of the singlet state.

Acknowledgment. This research was carried out with the support of the National Science Foundation. The calculations were performed on the Cray Y/MP at the Pittsburgh Supercomputing Center and on the Chemistry Department's FPS Model 500EA computer, funded by the NSF. We wish to thank Professor P. Dowd for many valuable discussions about diradical systems, Professor W. Borden for discussions of his work on TME, and Professor M. A. Robb for assistance with the use of the MCSCF routines in Gaussian 90.

Registry No. Tetramethyleneethane, 16893-57-5.

Theoretical Study of the Low-Lying Triplet and Singlet States of Diradicals. 2. Cyclopentadienyltrimethylenemethane

Petr Nachtigall, Paul Dowd, and Kenneth D. Jordan*

Contribution from the Department of Chemistry, University of Pittsburgh, Pittsburgh, Pennsylvania 15260. *Received September 23, 1991*

Abstract: Cyclopentadienyltrimethylenemethane has low-lying singlet and triplet states of A_1 and B_2 symmetry. The geometries of these states have been optimized by means of the ROHF, UHF, and MCSCF methods. The two lowest energy states—the $^3B_2$ ground state and the $^1A_1$ state, lying 4.9 kcal/mol above the ground state—are predicted to be planar. The higher-lying $^3A_1$ and $^1B_2$ states are found to have nonplanar structures.

Introduction

Nonalternant, non-Kekulé hydrocarbons have received relatively little attention from theory and none from an experimental standpoint. As a member of this class, cyclopentadienyltrimethylenemethane (CPTMM)[1] is expected to have low-lying singlet and triplet electronic states, with considerable diradical character. On the basis of Hückel MO calculations, it has been predicted that the ground state should be a singlet.[2,3] CPTMM has not been studied experimentally or by means of ab initio electronic structure methods.

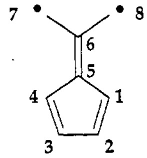

CP-TMM

CPTMM can be viewed as being derived from cyclopentadienyl and allyl fragments. Figure 1 presents a correlation diagram of the energies of the Hückel MO's of cyclopentadienyl, allyl, and CPTMM, and Figure 2 compares the Hückel energies and MO's of CPTMM and tetramethyleneethane (TME), a prototypical diradical.[4,5] At the Hückel level of theory CPTMM differs from TME in that the two frontier orbitals of TME are degenerate and nonbonding and also are energetically well separated from the other MO's, while for CPTMM the HOMO and the LUMO have rather different energies ($\alpha + 0.504\beta$ and α, respectively) and the second highest occupied orbital (SHOMO), with a Hückel energy of $\alpha + 0.618\beta$, is only slightly more stable than the HOMO. The symmetries of the three orbitals in question for CPTMM are: LUMO (a_2), HOMO (b_1), SHOMO (a_2), assuming a planar C_{2v} structure. As a consequence of the similar energies of the HOMO and SHOMO, CPTMM is expected to have low-lying $^3A_1$, $^1A_1$, $^3B_2$, and $^1B_2$ states.

The origin of the nearly degenerate a_2 SHOMO and b_2 HOMO in the Hückel model for CPTMM is readily apparent from consideration of the cyclopentadienyl plus allyl fragment model. The ground state of the allyl radical has a $1b_1^2 1a_2$ configuration, and cyclopentadienyl radical has two low-lying states, with $1b_1^2 2b_1^2 1a_2$ and $1b_1^2 1a_2^2 2b_1$ configurations. The degenerate $1a_2$ and $2b_1$ orbitals of the cyclopentadienyl fragment correlate with the $1a_2$ and $3b_1$ orbitals of CPTMM. Although the latter pair of orbitals are not degenerate, they lie close in energy providing all C–C bond lengths are assumed equal (as is done implicitly in the Hückel model).

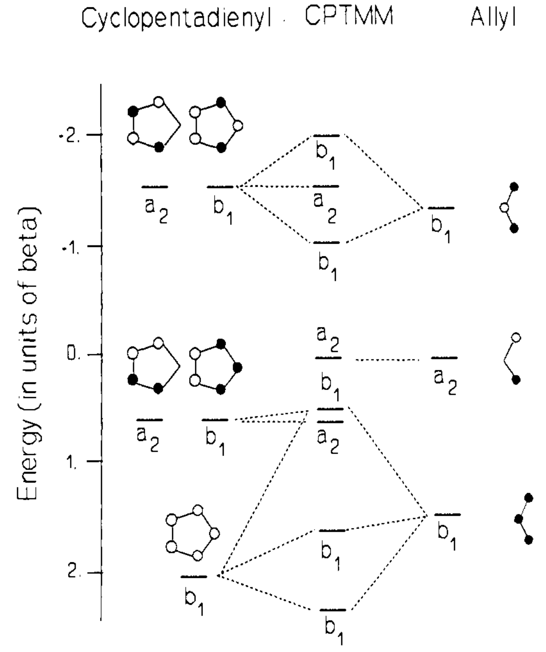

Figure 1. Correlation diagram showing the derivation of the π orbitals of CPTMM from the π orbitals of cyclopentadienyl and allyl radicals. Hückel orbital energies are employed.

The B_2 states of CPTMM, due to the $1b_1^2 1a_2^2 2b_1$ occupancy of the cyclopentadienyl fragment, should distort so as to stabilize the $1a_2$ MO and to destabilize the $3b_1$ MO (of CPTMM). Based on the MO's depicted in Figure 1, this should involve a shortening of the C_1–C_2 and C_3–C_4 bonds and a lengthening of the C_2–C_3 bond in the cyclopentadienyl fragment. Conversely, the A_1 states, due to the $1b_1^2 2b_1^2 1a_2$ occupancy of the cyclopentadienyl fragment,

---

(1) An alternative name for this compound is 2-(1′-cyclopentadienyl)allyl.

(2) Herndon, W. C.; Ellzey, M. L., Jr. *Tetrahedron Lett.* **1974**, 1399.

(3) Dowd, P. *Tetrahedron Lett.* **1991**, *32*, 445.

(4) Dowd, P.; Chang, W.; Paik, Y. H. *J. Am. Chem. Soc.* **1986**, *108*, 7416.

(5) Nachtigall, P.; Jordan, K. D. *J. Am. Chem. Soc.*, preceeding paper in this issue.

0002-7863/92/1514-4747$03.00/0

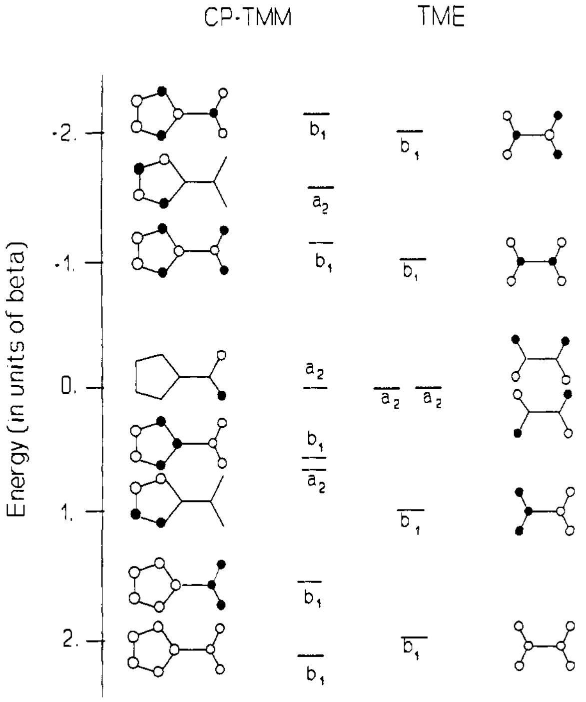

Figure 2. Hückel orbital energies and molecular orbitals of CPTMM and TME.

should distort so as to stabilize the $3b_1$ orbital and to destabilize the $1a_2$ orbital of CPTMM. These geometrical distortions should be in the opposite direction from those noted above for the B_2 states; namely, the C_1–C_2 and C_3–C_4 bonds should lengthen and the C_2–C_3 bond should shorten (relative to those in the model in which all C–C bond lengths are equal). All of these expectations are borne out by the multiconfiguration self-consistent field (MCSCF) calculations carried out in this study and discussed below.

The orbital energies for the $^3B_2$ and $^3A_1$ states of CPTMM, at the MCSCF optimized planar C_{2v} structures, are shown in Figure 3. For the $^3B_2$ state (Figure 3a), the lowest π orbitals are ordered $1b_1$, $2b_1$, $1a_2$, $3b_1$, $2a_2$ in terms of increasing energy, with the $3b_1$ and $2a_2$ orbitals being close in energy, whereas for the $^3A_1$ state (Figure 3b) the lowest π orbitals are ordered $1b_1$, $2b_1$, $3b_1$, $1a_2$, and $2a_2$, with the $1a_2$ and $2a_2$ orbitals being close in energy. The reversal of the order of the $1a_2$ and $3b_1$ orbitals in the two states is fully consistent with the prior discussion.

As shown in Figure 3, the π orbitals of CPTMM can also be viewed as being derived from those of *cis*-butadiene plus trimethylenemethane (TMM)[6] or from those of ethylene plus TME. The former model would lead one to expect the two frontier orbitals to be $3b_1$ and $2a_2$, i.e., the situation displayed in Figure 3a, and the latter model, in which CPTMM is derived from interacting ethylene and TME fragments, leads to a situation in which the two frontier orbitals are of a_2 symmetry as shown in Figure 3b.

The lowest energy $^3B_2$ and $^1B_2$ states of CPTMM should be well described by the $|...1a_2^2 3b_1^1 2a_2^1\rangle$ configuration and the lowest $^3A_1$ state by the $|...3b_1^2 1a_2^1 2a_2^1\rangle$ configuration.[7] The situation regarding the $^1A_1$ state is less clear cut as $|...3b_1^2 1a_2^1 2a_2^1\rangle$, $|...3b_1^2 1a_2^2\rangle$, and $|...3b_1^2 2a_2^2\rangle$ configurations are all possible. Based on the Hückel orbital energies (shown in Figure 2), CPTMM is expected to have a low-lying ionic state dominated by the $|...1a_2^2 3b_1^2\rangle$ π-electron configuration. This species would be well described as allyl (+)–cyclopentadienyl (–), and might be expected to be the ground state of CPTMM. Indeed, a geometry optimization with the $|...1a_2^2 3b_1^2\rangle$ Hartree–Fock wave function gives a structure with a dipole moment of 9.35 D. However, optimization of the geometry of the $^1A_1$ state in multiconfigurational treatments, even when starting with the ionic HF structure, gave rise to a relatively nonpolar ($\mu < 0.4$ D) structure, with the wave function being well described as ($|...3b_1^2 1a_2^2\rangle - |...3b_1^2 2a_2^2\rangle$). At first glance, it would appear that the relative nonpolarity of the $^1A_1$ state in the MCSCF approximation is due to nearly equal weights of configurations with allyl (+)–cyclopentadienyl(–) and allyl(–)–cyclopentadienyl(+) charge distributions. However, this is not correct; the $1a_2$ and $2a_2$ orbitals resulting from the MCSCF calculations are highly delocalized, and, as a result, the $^1A_1$ state of CPTMM, like that of TME, is actually covalent.[8]

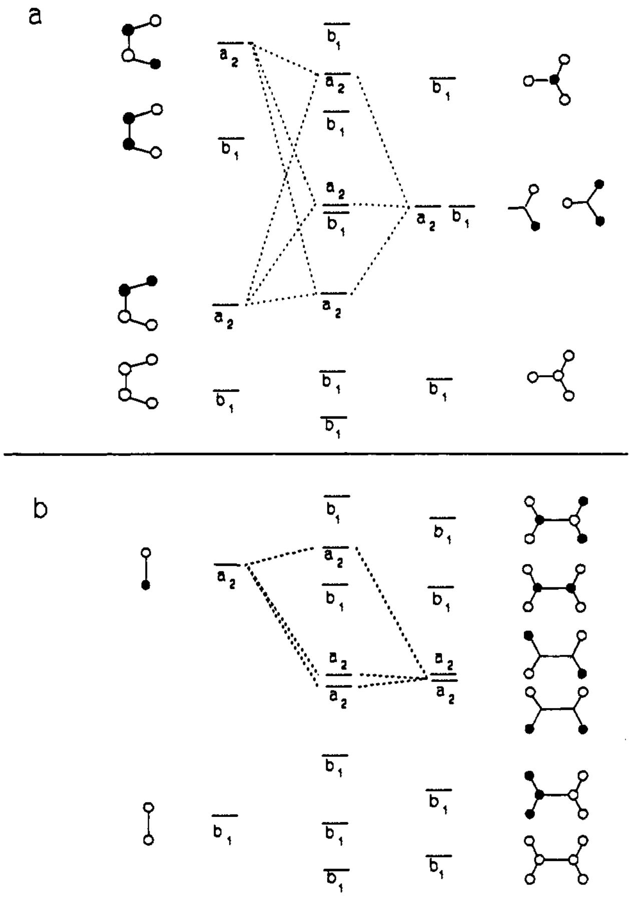

Figure 3. Correlation diagram showing the derivation of the π orbitals of CPTMM from (a) the π orbitals of the butadiene and trimethylenemethane and (b) the π orbitals of TME and ethylene. The orbital energies were obtained from HF calculations on ethylene, butadiene, TME, trimethylenemethane, and CPTMM using the geometry of the $^3A_1$ state (part b) and of the $^3B_2$ state (part a).

The $1a_2$ and $2a_2$ Hückel MO's of CPTMM are localized on opposite ends of the molecule. Thus, the exchange integral involving these orbitals should be quite small, and, as for the lowest singlet and triplet states of TME, the $^3A_1$ and $^1A_1$ states should be quite close in energy. The $3b_1$ orbital, on the other hand, is highly delocalized, and, as a result, the exchange integral involving this orbital and the $2a_2$ orbital should be sizable. This leads to the expectation that the $^3B_2$ state should lie energetically well below the $^1B_2$ state. Moreover, the $^3B_2$ state could lie energetically below the $^1A_1$ and $^3A_1$ states, making it the ground state.

The qualitative discussion presented above has assumed that CPTMM has a planar structure. In fact, one or more of the

---

[6] Dowd, P. *J. Am. Chem. Soc.* **1966**, *88*, 2587.

[7] Spin and antisymmetry have been ignored in specifying the various configurations in the text.

[8] For the $^1A_1$ state the MCSCF(2,2) procedure actually includes three configurations: $|...3b_1^2 1a_2^1 2a_2^1\rangle$, $|...3b_1^2 1a_2^2\rangle$, and $|...3b_1^2 2a_2^2\rangle$. However, these three configurations are not unique. In particular, MCSCF calculations with only the last two configurations give the same energy as that obtained from MCSCF calculations with the all three configurations. Also MCSCF calculations with only the first configuration give nearly the same energy as the three-configuration MCSCF. This is possible because the $1a_2$ and $2a_2$ orbitals localize in the MCSCF calculations employing only the first configuration, and they are delocalized in the MCSCF calculations employing only the second and third configurations listed above.

Table I. Calculated Energies (au) of the Triplet and Singlet States of CPTMM[a]

	$^1A_1$		$^3A_1$	
method[b]	I	II	I	II
UHF			−305.780 20	−305.785 80
MCSCF (2,2)	−305.744 68	−305.745 81	−305.743 84	−305.744 74
MCSCF(8,8)SD	−305.845 15	−305.842 84	−305.840 58	−305.841 45
MCSCF(8,8)	−305.856 28	−305.853 38	−305.851 17	−305.851 93
MCSCF(8,8)*	−307.570 25	−307.566 12	−307.565 20	−307.564 60

	$^1B_2$		$^3B_2$	
method[b]	I	II	I	II
UHF			−305.804 87	−305.792 12
MCSCF(2,2)			−305.764 14	−305.748 85
MCSCF(8,8)SD	−305.832 78	−305.841 81	−305.853 29	−305.841 45
MCSCF(8,8)	−305.842 79	−305.852 19	−305.864 64	−305.853 75
MCSCF(8,8)*		−307.565 19	−307.578 11	

[a] Structures I and II both have C_{2v} symmetry. Structure I is planar and structure II has the "allyl group" rotated 90° with respect to the plane of the ring. [b] The MCSCF(2,2) results are reported for the MCSCF(2,2)/3-21G optimized geometries, and the MCSCF(8,8) and MCSCF(8,8)SD calculations are carried out at the MCSCF(8,8)SD/3-21G optimized geometries. The calculations designated by * were carried out using 6-31G* basis set, employing the MCSCF(8,8)SD/3-21G optimized geometries.

low-lying electronic states could have nonplanar structures. In this work MCSCF calculations are carried out in order to develop a better understanding of the structures and relative stabilities of the low-lying $^1A_1$, $^3A_1$, $^1B_2$, and $^3B_2$ electronic states of CPTMM.

Computational Methodology

The geometries of the low-energy singlet and triplet states of CPTMM have been optimized by means of the MCSCF(2,2) and MCSCF(8,8)SD procedures employing the 3-21G basis set.[9] The geometries of the triplet states have also been optimized by means of the spin-unrestricted Hartree–Fock (UHF) method. The MCSCF(2,2) procedure distributes two active electrons in two active orbitals. In C_{2v} symmetry, the active orbitals are $1a_2$ and $2a_2$ for the A_1 states and $3b_1$ and $2a_2$ for the B_2 states. For the singlet states the MCSCF(2,2) procedure is equivalent to the two-configuration self-consistent field (TCSCF) method,[8] and for the triplet states it is equivalent to the restricted open-shell Hartree–Fock (ROHF) method. The MCSCF(8,8)SD procedure has eight active electrons in eight (four π and four π^*) orbitals. This procedure includes all symmetry-allowed single and double excitations in the active space generated from one reference configuration in the case of the $^3A_1$, $^3B_2$, and $^1B_2$ states and two reference configurations ($|...3b_1^2 1a_2^2\rangle$ and $|...3b_1^2 2a_2^2\rangle$) for the $^1A_1$ state.

The MCSCF(8,8)SD procedure is expected to give geometries very close to those which would be obtained from the MCSCF(8,8) procedure, which permits all arrangements of the electrons in the active space.[10] At selected MCSCF(8,8)SD/3-21G optimized geometries, MCSCF(8,8) calculations using the 3-21G and 6-31G* basis sets[11] were performed.

The UHF and MCSCF geometry optimizations were carried out with the Gaussian 90 program,[12] and the MCSCF(8,8) calculations were carried out with the UEXP program of Shepard and co-workers.[13]

Results and Discussion

A. Geometries. Three different geometries—planar (structure I), perpendicular (structure II), and twisted (structure III)—were considered. Both structures I and II have C_{2v} symmetry. In II, the plane of the allyl group is perpendicular to that of the cyclopentadienyl subunit. The twisted structure has C_2 symmetry. The A_1 and B_2 states of the C_{2v} structures correlate in C_2 symmetry with A and B states, respectively.

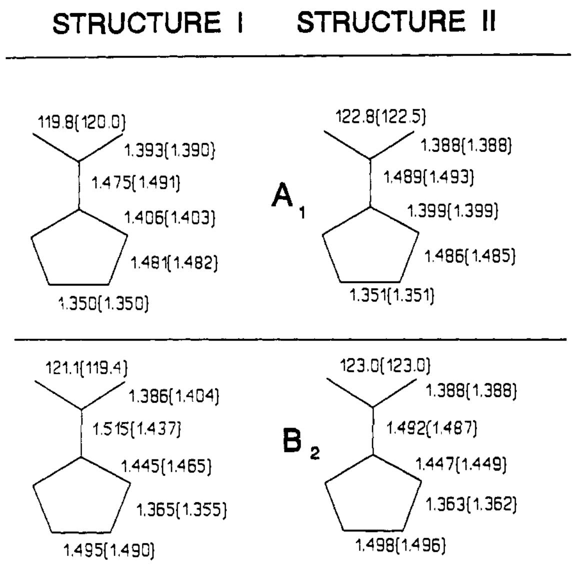

Figure 4. Geometries of CPTMM optimized at the MCSCF(8,8)SD/3-21G level of theory. The geometries for the planar (I) and perpendicular (II) structures are described on the left and on the right halves of the figure, respectively. The upper portion gives the parameters for the A_1 states and the lower portion for B_2 states. The results for both the singlet and triplet states are reported, with the latter values given in brackets. The bond lengths are in angstroms and the C_7–C_6–C_8 angles (α) in degrees.

MCSCF(2,2) calculations failed to give a C_2 minimum for the ^3B state, but rather converged to the planar C_{2v} structure. On the other hand, calculations at this level of theory do give C_2 structures for the ^3A and ^1A states, lying lower in energy than the corresponding perpendicular structures by 0.4 and 0.3 kcal/mol, respectively, and with an angle α between the planes of the cyclopentadienyl and allyl fragments of 45.3° and 43.8°, respectively. No attempt was made to optimize a C_2 structure for the ^1B state. Because the MCSCF(2,2) calculations show that the energy differences between the C_{2v} and C_2 structures are very small, the optimizations at the MCSCF(8,8)SD level of theory were carried out only for the C_{2v} structures. The ensuing discussion will focus on the results for the C_{2v} structures. The C_2 structures will be considered briefly toward the end of the paper.

The energies of the optimized structures are summarized in Table I. The values of most important geometrical parameters obtained at the MCSCF(8,8)SD/3-21G level of theory are reported in Figure 4. The geometrical parameters obtained for the A_1 states are reported in the upper portion of Figure 4, and those for the B_2 states are given in the lower portion of this figure. Structural parameters for the triplet states are given in brackets, following the parameters for the singlet states. For each symmetry type, the geometries of the singlet and triplet states are quite close. On the other hand, the geometries of A_1 states differ significantly from those of the B_2 states. In particular, the C_2–C_3 distance is about 0.14 Å shorter, the C_1–C_2 and C_3–C_4 distances are about 0.12 Å longer, and the C_1–C_5 and C_4–C_5 distances are about 0.05 Å shorter in the A_1 states than in the B_2 states. These results are consistent with the models discussed in the Introduction, where it was indicated that CPTMM, with a structure derived from TME and ethylene fragments, would favor the A_1 states, while a structure based on the *cis*-butadiene and the TMM radical fragments would favor the B_2 states. Unless specifically indicated otherwise, the geometries discussed in the text are those obtained in the MCSCF(8,8)SD approximation.

The valence-bond configurations that are important for the A_1 and B_2 states are schematically presented in Figure 5. The structures of the A_1 states are consistent with the domination of the valence-bond structures a and b which have a double bond between C_2 and C_3 and single bonds between C_1 and C_2 and between C_3 and C_4. In contrast, the B_2 states are dominated by valence bond structure d with a C_2–C_3 single bond and C_1–C_2 and C_3–C_4 double bonds. The C_1–C_5 and C_4–C_5 distances in the B_2

---

[9] Binkley, J. S.; Pople, J. A.; Hehre, W. J. *J. Am. Chem. Soc.* **1980**, *102*, 939.

[10] In ref 5 it was shown that the MCSCF(6,6)SD and MCSCF(6,6) procedures gave nearly the same geometries for the lowest singlet and triplet states of TME.

[11] Hehre, W. J.; Ditchfield, R.; Pople, J. A. *J. Chem. Phys.* **1972**, *56*, 2257. Hariharan, P. C.; Pople, J. A. *Theor. Chim. Acta* **1973**, *28*, 213.

[12] Frisch, M. J.; Head-Gordon, M.; Trucks, G. W.; Foresman, J. B.; Schlegel, H. B.; Raghavachari, K.; Robb, M. A.; Binkley, J. S.; Gonzalez, C.; Defrees, D. J.; Fox, D. J.; Whiteside, R. A.; Seeger, R.; Melius, C. F.; Baker, J.; Martin, R. L.; Kahn, L. R.; Stewart, J. J. P.; Topiol, S.; Pople, J. A., *Gaussian 90*; Gaussian, Inc., Pittsburgh, PA, 1990.

[13] Shepard, R.; Shavitt, I.; Simons, J. *J. Chem. Phys.* **1982**, *76*, 543. Brown, F. B.; Shavitt, I.; Shepard, R. *Chem. Phys. Lett.* **1984**, *105*, 363.

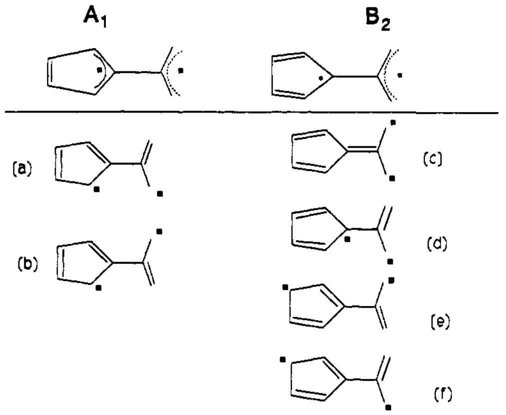

Figure 5. Valence bond (VB) structures important in the A_1 and B_2 states of CPTMM. In the case of energetically equivalent pairs of VB structures, only one member of the pair is shown. The VB structure (a) and (b) prove to be most important in the A_1 states, while the structure (d) is most important in the B_2 states. The VB structures (e) and (f) play a smaller, but still important, role in the B_2 states. VB structure (c) appears to play a small role in the $^3B_2$ state at its planar geometry.

Table II. Differences between the Structural Parameters Obtained Using the UHF and MCSCF(2,2) Procedures and Those Obtained at the MCSCF(8,8)SD Level of Theory[a]

	geometrical parameter					
method/state	C_5–C_6	C_6–C_7	C_1–C_5	C_1–C_2	C_2–C_3	α
ROHF/$^3B_2$	−0.017	−0.007	0.002	−0.013	−0.012	−0.1
UHF/$^3B_2$	0.004	0.006	−0.009	0.001	0.015	−0.2
(2,2)/$^1A_1$	0.010	−0.017	−0.012	−0.012	−0.006	−0.2

[a] Bond lengths are in angstroms and the angle α in degrees. A negative result denotes a bond length or angle smaller than that obtained with the MCSCF(8,8)SD approach.

states are about 1.45 Å, implying a small involvement of valence bond structures (probably e and f) which have double bonds between these atoms.

As noted above, the bond lengths of the singlet and triplet states of the same symmetry tend to be quite close. The most important exception is for the planar B_2 species for which the C_5–C_6 distance is about 0.070 Å shorter in the triplet than in the singlet state. In addition, the C_6–C_7, C_6–C_8, C_1–C_5, and C_4–C_5 distances are about 0.02 Å longer in the triplet state. These results suggest that the valence bond structure c in Figure 5 makes an important contribution to the wave function of the $^3B_2$ state in the planar configuration, but not to the wave function of the corresponding singlet state. We note also that the planar $^1A_1$ species has a C_5–C_6 distance about 0.015 Å shorter than does the planar $^3A_1$ species. This could be due to a small involvement of the $|\ldots 1a_2^2 2a_2^2\rangle$ configuration in the wave function of the planar $^1A_1$ state. The bond lengths in the planar and perpendicular structures are quite close, with the greatest differences being found for the C_5–C_6 distances (for the $^1A_1$, $^3B_2$, and $^1B_2$ states).

In general, the bond lengths and angles obtained at the MCSCF(8,8)SD level of theory are fairly close to those obtained by means of the MCSCF(2,2) method. This may be seen for the $^1A_1$ and $^3B_2$ states from the results summarized in Table II. Interestingly, for the $^3B_2$ state the deviations of the MCSCF(2,2) and UHF bond lengths from the MCSCF(8,8)SD values are in opposite directions. Comparable differences between the MCSCF(2,2) and MCSCF(8,8)SD geometries are found for the $^3A_1$ state, the results for which have not been included in Table II.

It was observed in the Introduction that for the A_1 states the π orbitals can be viewed as being derived from those of ethylene plus TME. Thus, it is of interest to note that the C_2–C_3 bond length calculated for both the $^3A_1$ and $^1A_1$ states is about 1.35 Å, close to the C–C bond length of ethylene (1.315 Å), optimized in the MCSCF(2,2)/3-21G approximation. Moreover, the C_5–C_6 bond lengths of the $^1A_1$ and $^3A_1$ states of planar CPTMM (1.475 Å and 1.491 Å, respectively) correlate fairly well with the C_1–C_2 bond length of planar TME determined at the MCSCF(6,6)/3-21G level of theory (1.498 Å and 1.514 Å for the singlet and triplet states, respectively). Similarly, for the B_2 states of CPTMM, the C_2–C_3 bond length of CPTMM is close to the C_2–C_3 bond length of butadiene, and the C_1–C_2 and C_3–C_4 bond lengths of CPTMM are close to those of the terminal C–C bonds of butadiene.

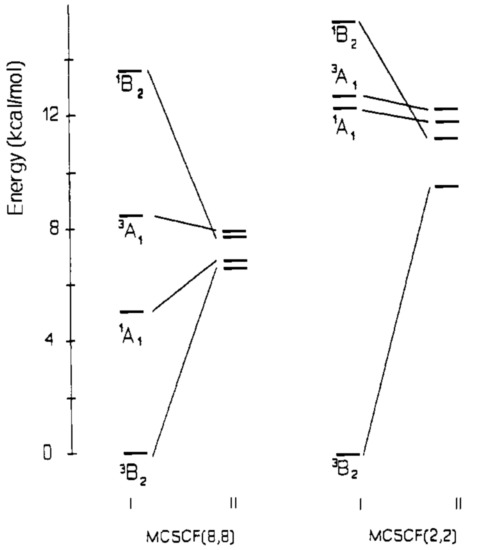

Figure 6. Relative energies (in kcal/mol) of the low-lying states of CPTMM for the planar (I) and perpendicular (II) structures. The results obtained by means of the MCSCF(8,8)/3-21G and MCSCF-(2,2)/3-21G approaches are given in the left- and right-hand sides of the figure, respectively.

B. Relative Energies. Figure 6 presents a correlation diagram of energies of the four states in their planar and perpendicular structures. The left-hand side of the figure reports the MCSCF(8,8)/3-21G energies, and the right-hand side reports the MCSCF(2,2)/3-21G energies. The former are calculated at the MCSCF(8,8)SD/3-21G geometries and the latter at the MCSCF(2,2)/3-21G geometries.[14] The energies (in kcal/mol) are reported relative to that of the planar $^3B_2$ state at the respective level of theory.

From Figure 6 it is seen that, at both the MCSCF(2,2) and MCSCF(8,8) levels of theory, the four states are energetically well separated for the planar geometries, but that they lie close in energy for the perpendicular structures. At both levels of theory the four states in their planar structures are ordered $^3B_2$, $^1A_1$, $^3A_1$, and $^1B_2$ in terms of increasing energy. For the perpendicular structures, both levels of theory place the $^3B_2$ state lowest in energy and the $^3A_1$ state highest in energy. However, the ordering of the closely spaced $^1A_1$ and $^1B_2$ states in their perpendicular structures is different in the two approximations, with the $^1A_1$ state being lower in energy in the MCSCF(8,8) approximation. Both levels of theory place the planar form of the $^3B_2$ state energetically below the perpendicular form and also indicate that the $^3A_1$ and $^1B_2$ states prefer the perpendicular over the planar structure.

There are other important differences between the results obtained at the two levels of theory. The most significant are enumerated here. Firstly, the MCSCF(2,2) calculations give much larger energy separations between the $^3B_2$ state and the other states (particularly, for the planar structures) than do the MCSCF(8,8) calculations. Secondly, the MCSCF(2,2) calculations predict the perpendicular form of the $^1A_1$ state to be energetically below the planar structure, contrary to the MCSCF(8,8) calculations.

We now examine in closer detail the relative energies of the various species as described at the MCSCF(8,8)/3-21G level of theory. The $^3B_2$ state in its planar structure lies 6.8 kcal/mol below

---

(14) Because of convergence difficulties, the geometry of the $^1B_2$ state of CPTMM was not optimized at the MCSCF(2,2) level of theory. The MCSCF(2,2) energies reported in Figure 6 for planar and perpendicular forms of the $^1B_2$ state are calculated using the MCSCF(8,8)SD/3-21G optimized geometries.

Table III. Natural Orbital Occupations from MCSCF(8,8) Calculations with the 3-21G Basis Set

	$^1A_1$		$^3A_1$		$^1B_2$		$^3B_2$	
orbital[a]	I	II	I	II	I	II	I	II
$5b_1$	0.06	0.09	0.07	0.09	0.07	0.08	0.06	0.08
$3a_2$	0.08	0.08	0.08	0.08	0.09	0.09	0.08	0.09
$4b_1$	0.15	0.10	0.13	0.10	0.10	0.10	0.12	0.10
$2a_2$	0.88	0.89	1.00	1.00	1.00	1.00	1.00	1.00
$1a_2$	1.14	1.12	1.01	1.01	1.89	1.89	1.89	1.89
$3b_1$	1.84	1.89	1.86	1.89	1.01	1.01	1.01	1.01
$2b_1$	1.92	1.90	1.91	1.90	1.91	1.90	1.90	1.90
$1b_1$	1.94	1.93	1.93	1.93	1.93	1.93	1.94	1.93

[a] The orbital symmetries are those for the planar C_{2v} structure (I).

Table IV. Relative Energies (kcal/mol) of the Low-Lying Electronic States of CPTMM[a]

		$^3B_2$		$^1B_2$	
method	basis set	I	II	I	II
MCSCF(8,8)SD	3-21G	0.0	7.4	12.9	7.2
MCSCF(8,8)	3-21G	0.0	6.8	13.7	7.8
MCSCF(8,8)[b]	6-31G*	0.0			8.1

		^3A			^1A		
method	basis set	I	II	III	I	II	III
MCSCF(2,2)	3-21G	12.7	12.2	11.9	12.2	11.5	11.1
MCSCF(8,8)SD	3-21G	8.0	7.4	6.6	5.1	6.6	5.6
MCSCF(8,8)	3-21G	8.5	8.0	7.3	5.2	7.1	7.7
MCSCF(8,8)[b]	6-31G*	8.1	8.5		4.9	7.5	

[a] Energies relative to that of structure I of the $^3B_2$ state at the particular level of theory. [b] MCSCF(8,8) calculations with the 6-31G* basis set were carried out only for the $^3B_2$ (structure I), $^1B_2$ (structure II), $^3A_1$ (structures I and II), and $^1A_1$ (structures I and II) states.

the perpendicular structure. (Vibrational frequency calculations carried out at the UHF/3-21G level of theory for the $^3B_2$ state confirm that the planar structure is a minimum and the perpendicular structure is a saddle point.) The first excited state is the $^1A_1$ state, which, at this level of theory, also prefers a planar structure, with the planar structure being about 1.8 kcal/mol more stable than the perpendicular structure. The energy separation between the $^3B_2$ and $^1A_1$ states at their respective planar structures is 5.25 kcal/mol. The other two states, $^3A_1$ and $^1B_2$, prefer perpendicular structures. For the $^3A_1$ state the perpendicular structure lies only 0.5 kcal/mol below the planar structure, while for the $^1B_2$ state, the perpendicular structure is favored by 5.9 kcal/mol. The potential for rotation about the C_5–C_6 bond is rather shallow for both the triplet and singlet A_1 states. The larger energy changes in the B_2 states than in the A_1 states upon going from the planar to the perpendicular structures is consistent with the larger exchange integral for two frontier orbtials in the B_2 states.

C. Natural Orbital Occupations. The natural orbital (NO) occupation numbers obtained from the MCSCF(8,8)/3-21G wave functions for all four low-lying states are summarized in Table III. For the B_2 states the NO occupation numbers are nearly identical for the singlet and the triplet as well as for structures I and II. On the other hand, there are significant differences between the NO occupation numbers of the $^3A_1$ and $^1A_1$ states and between the two structures for both the $^3A_1$ and $^1A_1$ states. The $^1A_1$ and $^3A_1$ states have appreciably different occupation numbers for the $1a_2$ and $2a_2$ orbitals, with the occupation numbers for these two orbitals being nearly identical (and close to 1.00) for the triplet state, and differing by 0.23–0.26 for the ^1A states. This is consistent with the greater importance of the $|...3b_1^2 1a_2^2\rangle$ configuration than the $|...3b_1^2 2a_1^2\rangle$ configuration in the $^1A_1$ state. The occupation of the $3b_1$ NO is smaller and that of $4b_1$ NO larger in the planar than in the perpendicular structures for the $^3A_1$ and $^1A_1$ states, with the difference being slightly greater for the $^1A_1$ state. This is consistent with the fact that electron correlation is more important for the planar $^1A_1$ species than for the perpendicular $^1A_1$ species or for either structure for the $^3A_1$ state.

D. 6-31G* Versus 3-21G Basis Sets. For each of the four low-lying states of CPTMM, MCSCF(8,8)/3-21G and MCSCF(8,8)/6-31G* calculations were performed at the MCSCF(8,8)SD/3-21G optimized geometries. Total energies from these calculations are summarized in Table I, and energies relative to the $^3B_2$ planar species are summarized in Table IV. As expected, the relative energies obtained at the MCSCF(8,8)SD/3-21G and MCSCF(8,8)/3-21G levels of theory are nearly the same. The inclusion of d polarization functions in the basis set also proves to be relatively unimportant for the relative energies, an exception being the $^3A_1$ state, for which the MCSCF(8,8) calculations with the 3-21G basis set predict the perpendicular structure to be 0.5 kcal/mol below the planar structure, while those with the 6-31G* basis set place the planar structure 0.4 kcal/mol below the perpendicular structure.

E. C_2 Structures. It was mentioned at the beginning of this section that MCSCF(2,2)/3-21G calculations predict the ^1A and ^3A states to be slightly more stable (by 0.3 and 0.4 kcal/mol, respectively) in the C_2 than in their perpendicular C_{2v} structures. With the exception of the dihedral angle, the geometries obtained for the twisted C_2 species are very close to those of the corresponding perpendicular structures. The greatest differences are in the C_5–C_6 bond lengths, which in the C_2 structures are about 0.007 Å shorter than in the perpendicular structures and, in fact, are very close to those found for the planar structures.

MCSCF(8,8)SD and MCSCF(8,8) calculations using the 3-21G basis set have also been performed for the ^3A and ^1A states using estimated C_2 geometries. In these calculations the geometries of the C_2 species are taken to be the same as for structure II, but with the C_5–C_6 bond lengths shortened to the values found for structure I, and the twisting angle θ taken to be 45.0°. The relative energies of the various structures at different levels of theory are summarized in Table IV. Since the MCSCF(8,8)SD and MCSCF(8,8) calculations give similar results, only the latter will be considered in the following discussion.

For the $^3A_1$ state, both the MCSCF(8,8) and MCSCF(2,2) calculations place the C_2 structure slightly lower in energy than the perpendicular structure. However, we saw above that for the $^3A_1$ state the inclusion of d functions caused structure I to be favored over structure II, and it is possible that MCSCF(8,8) calculations with the 6-31G* basis set would fail to give a C_2 minimum for the ^3A species. For the $^1A_1$ state, the MCSCF(8,8)/3-21G calculations place the planar (structure I) below the C_2 structure (by 0.7 kcal/mol), in contrast to the MCSCF(2,2) calculations. It is possible that geometry optimizations at the MCSCF(8,8)SD level of theory would locate a C_2 form of the $^1A_1$ state slightly below the planar C_{2v} structure. More extensive calculations are required in order to definitively establish whether the ^{3}A and ^{1}A states of CPTMM have potential energy minima of C_2 symmetry. In any case, it is clear that twisting potentials of the ^{3}A and ^{1}A states of CPTMM are quite shallow.

F. Vertical Excitation Energies. The vertical excitation energies for CPTMM have been calculated at the MCSCF(8,8)/3-21G level of theory. For the $^3B_2$ species the predicted vertical excitation energies are 16.7, 27.9, and 32.2 kcal/mol for the transitions into $^1B_2$, $^1A_1$, and $^3A_1$ states, respectively. For the $^1A_1$ species vertical excitation energies of 3.2, 17.4, and 29.5 kcal/mol are predicted for the transitions into $^3A_1$, $^3B_2$, and $^1B_2$ states, respectively. Because of the large geometry differences between the A and B states, the state orderings as deduced from the vertical excitation spectra differ from those given in Figure 6, in which the energy of each state is reported at the optimized structure for that state.

Conclusions

The geometries of the lowest singlet and triplet states of CPTMM have been optimized by means of the UHF, MCSCF(2,2), and MSCSF(8,8)SD methods. The ground state of CPTMM is predicted to be $^3B_2$ and the first excited state to be $^1A_1$, with the $^3B_2$ state lying 4.9 kcal/mol below the $^1A_1$ state at the MCSCF(8,8)/6-31G* level of theory. Both of these states are found to be planar (at the MCSCF(8,8) level of theory). For the $^3B_2$ state there is a large (6.8 kcal/mol at the MCSCF(8,8)/3-21G level of theory) rotational barrier. On the other hand, the barrier for rotation in the $^1A_1$ state is predicted to be appreciably smaller (1.8 and 2.6 kcal/mol at the MCSCF(8,8)/3-21G and MCSCF(8,8)/6-31G* levels of theory, respectively).

The $^1A_1$ and $^3A_1$ states of CPTMM are closely analogous to the lowest energy singlet and triplet states of TME. In both cases the lower energy state is predicted to be a singlet. For CPTMM the $^1A_1$ state is predicted to be 2.8 kcal/mol below the $^3A_1$ (MCSCF(8,8)/3-21G results), whereas for TME the singlet is predicted to lie 1.3 kcal/mol below the triplet state (MCSCF(6,6)/3-21G results). For both TME and CPTMM the twisting potentials are quite shallow.

Electron correlation effects are found to be very important for predicting the spacing between the $^3B_2$ and $^1A_1$ states of CPTMM. However, the differences in the geometries as predicted in the MCSCF(2,2) and MCSCF(8,8)SD approximations are relatively unimportant for the state separation: in fact, MCSCF(8,8) calculations give nearly the same energy separation between the $^3B_2$ and $^1A_1$ states regardless of whether the MCSCF(2,2) or MCSCF(8,8)SD optimized geometries are employed.

All four states ($^1A_1$, $^3A_1$, $^3B_2$, and $^1B_2$) of CPTMM considered here are relatively nonpolar (with a dipole moments less than 0.4 D). Although an ionic allyl(+)–cyclopentadienyl(−) $^1A_1$ species is found in the HF approximation, the lowest $^1A_1$ state optimized by means of the MCSCF procedure is relatively nonpolar.

Acknowledgment. This research was supported by grants from the National Science Foundation (K.D.J. and P.D.). The calculations were performed on the Cray YMP at the Pittsburgh Supercomputing Center and on the FPS Model 500EA computer in the Chemistry Department at the University of Pittsburgh. We wish to thank Professor M. A. Robb for his assistance in the use of the MCSCF portion of Gaussian 90, and Professor W. Borden for helpful suggestions concerning the manuscript.

Registry No. CP-TMM, 55524-34-0.

Theoretical Calculations on 1,2-Ethanediol. 2. Equilibrium of the Gauche Conformers with and without an Intramolecular Hydrogen Bond in Aqueous Solution

Peter I. Nagy,† William J. Dunn, III,* Giuliano Alagona,* and Caterina Ghio

Contribution from the College of Pharmacy, P.O.B. 6998, The University of Illinois at Chicago, Chicago, Illinois 60680, and the Istituto di Chimica Quantistica ed Energetica Molecolare del C.N.R., Via Risorgimento 35, I-56126 Pisa, Italy. *Received June 21, 1991*

Abstract: Ab initio calculations were carried out on the tGg, tGt, and gGg conformers of 1,2-ethanediol in the gas phase and then Monte Carlo simulations were carried out in aqueous solution. MP2/6-31G*//6-31G* results with zero-point and thermal corrections (T = 298 K) show that these conformers without intramolecular hydrogen bonding are higher in free energy by 3–4 kcal/mol than the most stable tGg′ conformer. Hydration of the tGg conformer leads to stabilization by 5.2 kcal and is the most likely conformer in aqueous solution. It represents 64% of the conformer population considering tGg, gGg′, tGg′, tGt, tTt, and gGg conformers. This finding of the tGg-dominant conformer with a gauche O–C–C–O linkage and without intramolecular hydrogen bonding fits well with NMR and Raman experiments for the solution. The polar groups of the solute are hydrated by five to seven water molecules and form about four hydrogen bonds with them. The most stable bonds are nearly linear O–H(alc)···O(water) arrangments. Hydrogen bonds to O(alc) with donor water molecules exhibit less defined geometry. Water molecules hydrating the gauche hydroxyl group are more strictly localized than those for a trans one. The number of water molecules in the nonpolar region is not effected by conformational changes of the solute considering rotation either about the C–C axes or about the C–O bonds.

Introduction

1,2-Ethanediol is a very simple example of a system with possible intramolecular hydrogen bonds due to vicinal polar groups. Formation of an internal hydrogen bond in a gauche O–C–C–O conformation may be favorable, while the trans arrangement prohibits that formation. In our previous report[1] (part 1), we focused on studying the gauche–trans equilibrium of 1,2-ethanediol as the major conformational change of the molecule. To this end the most stable gauche and trans conformations, determined by

---

* To whom correspondence should be addressed.

† On leave from Chemical Works of Gedeon Richter Ltd., Budapest, Hungary.

(1) Nagy, P. I.; Dunn, W. J., III; Alagona, G.; Ghio, C. *J. Am. Chem. Soc.* **1991**, *113*, 6719.

0002-7863/92/1514-4752$03.00/0